Description of Scattering Object

A homogeneous lossy magneto-dielectric plate of size $W \times 7W/4 \times 1.5$ mm.

Length Scale and Frequency Range

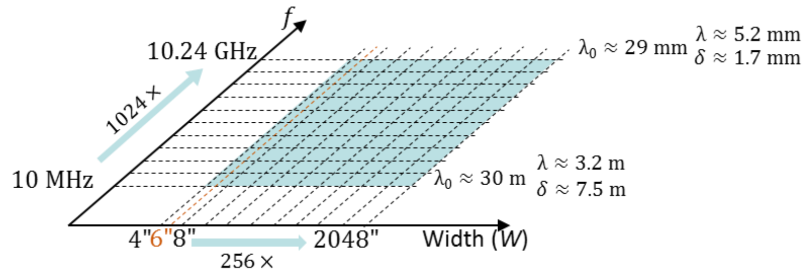

The problems of interest cover a range of 512x in physical length scale and 1024x in frequency; the ranges are logarithmically sampled to yield 110 scattering problems. Because of the extra data for the $W = 6$ in plate, there are 110 + 12 unique scattering problems in Problem Set IID. In these problems, the plate sizes are in the range $0.0033 \le W/\lambda_0 \le 1776$ and $1.3 \times 10^{-2} \le W/\delta \le 3.2 \times 10^4$, where λ_0 is the free-space wavelength and δ is the penetration depth in the magnetic radar absorbing (MagRAM) material. The length and width of the plates were chosen to approximately match the plate targets in [1], while the thickness was chosen to match an available sample of the ARC Technologies' DD-13490, a flexible silicone rubber microwave absorber [2].

Interesting Features

1. The logarithmic sampling is distorted along the length axis and an extra plate of $W = 6$ in is introduced because of publicly available measurement data corresponding to this size [3]. The sampling is also distorted along the frequency axis: scattering from the plate of $W = 6$ in at frequencies $f \in$ {10, 20, 40, 80, 160, 320, 640, 1280, 2560, 5120, 7000, 10240} MHz are included in the problem set because of publicly available measurement data [3]. These distortions add 12 unique scattering problems to the set.
2. The thin side wall presents meshing and accurate integration challenges.
3. The lossy magneto-dielectric material introduces extra uncertainties and sensitivities to RCS measurements and simulations [4].

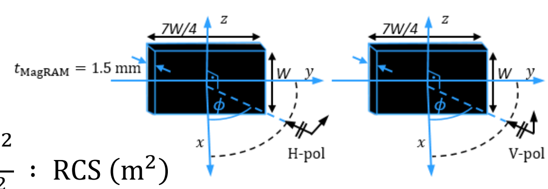

Quantities of Interest

Radar cross section (RCS) definition

$$\sigma_{vu}(\theta^{\rm s},\phi^{\rm s},\theta^{\rm i},\phi^{\rm i}) = \lim_{R\to\infty} 4\pi R \frac{|\hat{v}(\theta^{\rm s},\phi^{\rm s})\cdot \mathbf{E}^{\rm scat}(\theta^{\rm s},\phi^{\rm s})|^2}{|\hat{u}(\theta^{\rm i},\phi^{\rm i})\cdot \mathbf{E}^{\rm scat}(\theta^{\rm i},\phi^{\rm i})|^2} \quad : \ \text{RCS (m}^2)$$

$$\sigma_{vu,\rm dB}(\theta^{\rm s},\phi^{\rm s},\theta^{\rm i},\phi^{\rm i}) = 10\log_{10}\sigma_{vu} \quad : \ \text{RCS in dB (dBsm)}$$

$$\sigma^{TH}_{vu,\rm dB}(\theta^{\rm s},\phi^{\rm s},\theta^{\rm i},\phi^{\rm i}) = \max\left(\sigma_{vu,\rm dB}, TH_{vu,\rm dB}\right) - TH_{vu,\rm dB} \quad : \ \text{Thresholded RCS}$$

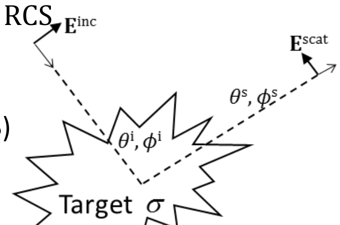

1. Set $\theta^{\rm i} = 90^{\rm o}$. Vary $0^{\rm o} \le \phi^{\rm i} \le 90^{\rm o}$ (every $0.5^{\rm o}$ in the interval).
2. Compute back-scattered $\sigma_{\theta\theta,\rm dB}$ and $\sigma_{\phi\phi,\rm dB}$ (the VV- and HH-pol RCS in dB) at $N_\phi = 181$ scattering directions.

Material Properties

Debye models expressed as $\epsilon(f) = \epsilon_0\varepsilon_r(f)$ and $\mu(f) = \mu_0\mu_r(f)$, where

$$\varepsilon_r(f) = \varepsilon_r'(f) - j\varepsilon_r''(f) = 16.92 - j0.33447 + \frac{0.0168 - j0.00464}{1 + jf(0.05093 + j0.2051)}$$

$$\mu_r(f) = \mu_r'(f) - j\mu_r''(f) = 0.35 - j0.1307 + \frac{3.865 - j0.6854}{1 + jf(0.1403 - j0.041)}$$

were used to calculate the complex permittivity and permeability of the MagRAM at the frequencies of interest. The reference simulation results were computed using precisely the permittivity and permeability values (i.e., to machine precision) shown in the below table. The above Debye models for the MagRAM are slightly different than that in [3] and were obtained by fitting to the data in the spec sheet of the material. Simulations using these values were found to yield better agreement with the measured RCS values.

Frequency f (MHz)	ϵ'	ϵ''	μ'	μ''
10	16.9	0.339	4.21	0.821
20	16.9	0.339	4.21	0.826
40	16.9	0.339	4.20	0.837
80	16.9	0.339	4.19	0.857
160	16.9	0.339	4.17	0.897
320	16.9	0.340	4.13	0.975
640	16.9	0.341	4.03	1.12
1280	16.9	0.343	3.81	1.37
2560	17.0	0.353	3.33	1.72
5120	16.9	0.393	2.46	1.95
7000	16.9	0.347	1.99	1.92
10 240	16.9	0.337	1.45	1.73

Performance Measures

Error Measure: Simulation errors shall be quantified using

$$avg.err_{uu,\text{dB}}^{TH} = \frac{1}{2\pi}\int_0^{2\pi} \left|\sigma_{uu,\text{dB}}^{TH}(\phi^s) - \sigma_{uu,\text{dB}}^{\text{ref},TH}(\phi^s)\right| d\phi^s \approx \frac{1}{N_\phi}\sum_{n=1}^{N_\phi}\left|\sigma_{uu,\text{dB}}^{TH}(\phi_n^s) - \sigma_{uu,\text{dB}}^{\text{ref},TH}(\phi_n^s)\right| \ \text{(dB)} \ \text{ for } u \in \{\theta,\phi\}$$

where

$$TH_{uu,\text{dB}} = \max_{\phi^s} \sigma_{uu,\text{dB}}^{\text{ref}} - 80 \ \text{(dB)}$$

This error measure discounts errors in RCS values smaller than TH.

Cost Measure: Simulation costs shall be quantified using observed wall-clock time and peak memory/process

$$t^{\text{wall}}\text{(s) and } mem^{\text{maxproc}}\text{(bytes)}$$

as well as the "serialized" CPU time and total memory requirement

$$t^{\text{total}} = N_{\text{proc}} \times t^{\text{wall}}\text{(s) and } mem^{\text{max}} = N_{\text{proc}} \times mem^{\text{maxproc}} \text{ (bytes)}$$

Here, N_{proc} denotes the number of processes used in a parallel simulation. It is expected that results will be reported for at least 2 runs: "Efficient" (small N_{proc}) and "Fast" (large N_{proc}).

Study 1: Error vs. Cost Sweep

Fix frequency and fix plate dimensions. Simulate many error levels (proxy: mesh densities) for 4 cases:

Case 1: *f*=10 MHz, *W*=6 in

Case 2: *f*=7 GHz, *W*=6 in (a measurement frequency)

Case 3: *f*=10 MHz, *W*=128 in

Case 4: *f*=320 MHz, *W*=128 in

It's recommended to simulate as many error levels (mesh densities) as possible. 3-5 error levels is typical. A typical error-vs.-cost study will consist of 4x3-5=12-20 simulations.

Study 2: Frequency Sweep

Fix plate dimensions and error level (proxy: mesh density). Simulate many frequencies for 4 cases:

Case 1: *W*=6 in, error level 1 (coarsest mesh)

Case 2: *W*=128 in, error level 1 (coarsest mesh)

Case 3: *W*=6 in, error level 2 (finer mesh)

Case 4: *W*=128 in, error level 2 (finer mesh)

Frequencies shall be chosen as $f \in \{10, 20, 40, \ldots, 5120, 10240\}$ MHz. It's recommended to simulate as many frequencies as possible. A full frequency-sweep study will consist of 4x11=44 simulations.

Study 3: Size Sweep

Fix frequency and error level (proxy: mesh density). Simulate many sizes for 4 cases:

Case 1: f=10 MHz, error level 1 (coarsest mesh) Case 2: f=320 MHz, error level 1 (coarsest mesh)

Case 3: f=10 MHz, error level 2 (finer mesh) Case 4: f=320 MHz, error level 2 (finer mesh)

Dimensions shall be chosen as $W \in \{4, 8, 16, \dots, 1024, 2048\}$ in. It's recommended to simulate as many sizes as possible. A full size-sweep study will consist of 4x10=40 simulations.

Reference Quantities of Interest

The following RCS data are made available in the benchmark to enable participants to calibrate their simulators:

4 RCS measurement results corresponding to the W=6 in plate at frequencies $f \in \{2560, 5120, 7000, 10240\}$ MHz. They are provided for ϕ^{i} sampled every 0.25^{o}.

4 RCS simulation results for the W=6 in plate at the above 4 frequencies found by using the ARCHIE-AIM code, a frequency-domain FFT-accelerated integral-equation solver developed at UT Austin [5]-[7].

References

[1] A. C. Woo, H. T. G. Wang, M. J. Schuh and M. L. Sanders, "EM programmer's notebook-benchmark radar targets for the validation of computational electromagnetics programs," *IEEE Ant. Propag. Soc. Mag.*, vol. 35, no. 1, pp. 84-89, Feb. 1993.

[2] ARC Technologies, "Technical Data Sheet DD-13490. [Online]. Available: http://arc-tech.com/pdf/DD-13490%20Rev%20C.pdf

[3] J. T. Kelley, D. A. Chamulak, C. Courtney, and A. E. Yilmaz, "Increasing the material diversity in the Austin RCS Benchmark Suite using thin plates," in *Proc. Ant. Meas. Tech. Assoc. (AMTA) Symp.*, Nov. 2020.

[4] J. T. Kelley, B. MacKie-Mason, D. A. Chamulak, M. Martin, K. Crouch, C. C. Courtney, and A. E. Yilmaz, "Towards quantifying the effect of material uncertainty on RCS predictions of composite targets," in *Proc. ACES Symp.*, May 2024.

[5] M. F. Wu, G. Kaur, and A. E. Yılmaz, "A multiple-grid adaptive integral method for multi-region problems," *IEEE Trans. Antennas Propag.*, vol. 58, no. 5, pp. 1601-1613, May 2010.

[6] F. Wei and A. E. Yılmaz, "A more scalable and efficient parallelization of the adaptive integral method part I: algorithm," *IEEE Trans. Antennas Propag.*, vol. 62, no. 2, pp. 714-726, Feb. 2014.

[7] J. W. Massey, V. Subramanian, C. Liu, and A. E. Yılmaz, "Analyzing UHF band antennas near humans with a fast integral-equation method," in *Proc. EUCAP*, Apr. 2016.